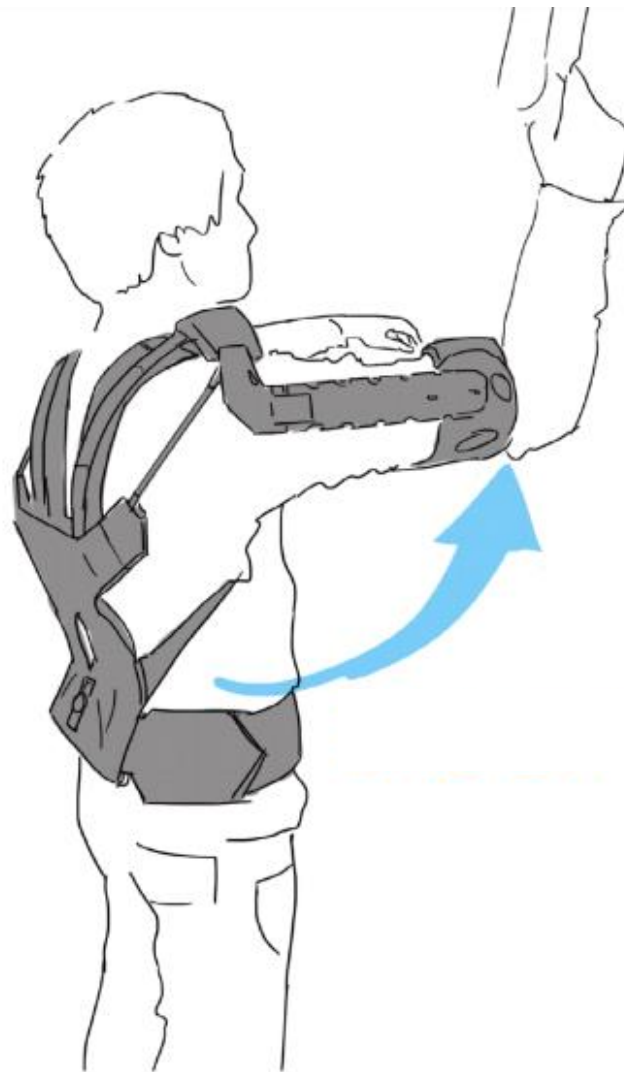


Modeling and altering the force profile of a spring-based upper body exoskeleton with design adjustments

I.J. de Looij

Master of Science Thesis



Modeling and altering the force profile of a spring-based upper body exoskeleton with design adjustments

by

Ivo J. de Looij

For the degree of Master of Science in Mechanical Engineering
at Delft University of Technology.

Student number: 4076931
Department : Biomechanical Design
Project duration: December 1, 2016 – August 9, 2017

Thesis committee: Dr. Ir. D.A. Abbink Supervisor, TU Delft
Dr. Ir. P. Lambert, Supervisor, TU Delft
Dr. Ir. V. van der Wijk External Member, TU Delft

An electronic version of this thesis is available at <http://repository.tudelft.nl/>.



Copyright © Biomechanical Engineering
All rights reserved.

Acknowledgements

This paper is the result of 8 months of analyzing, programming, building, testing writing and rewriting. In this dedicated section I would like to thank the ones that helped me along the way.

First of all, I would like to thank my daily supervisor Patrice Lambert. The discussion and analyzes were very helpful and pushed me in the right direction. Thanks to my supervisor David Abbink for his critical questions during the joint supervision sessions that helped me shape my research and my paper.

Thanks to Gaurav Genani, the founder and CEO of SkelEx, for the opportunity to do this thesis at SkelEx. Thanks for the critical questions, they helped developing new ideas.

Thanks to the SkelEx team, first of all with the brainstorm sessions but mostly with the welcome entertainment. Thanks for the lively discussions about life and the universe. Also thanks for including me in the brainstorm sessions about the future of the company.

Thanks to Sjors Oudshoorn and Elco Heijmink for the feedback on my paper as well as listening to the challenges I had to overcome to get to this paper.

Furthermore, thanks to the members of the Haptics lab for letting me distract everyone. This was for me the place to go, outside of the Skel-Ex cave.

I also would like to thank my family for supporting me over the years. Without you, this all wouldn't be possible.

And finally I would like to thank Marion for the patience the last months and the needed distraction.

Thank you all for the support during this intense period.

Ivo de Looij
Delft University of Technology
Delft, August 2017

Preface

The SkelEx exoskeleton is developed to support workers with work above or in front of the head. This work presents methods for adjusting the output force of this novel exoskeleton system; a finite element model was build together with experimental setups to evaluate and validate the force at different angles of the upper arm .

This thesis, titled 'Modeling and altering the force profile of a spring-based upper body exoskeleton with design adjustments', is submitted as part of the degree of Master of Science in Biomechanical Design, at the Delft University of Technology, The Netherlands. The research described herein was conducted under the supervision of Dr. Ir. D.A. Abbink and Dr. Ir. P. Lambert of the Department of Biomechanical Engineering, Haptic Interfaces and the Department of Precision and Microsystems Engineering, at the Faculty of Mechanical, Maritime and Materials Engineering, Delft.

Ivo de Looij
Delft University of Technology
Delft, August 2017

CONTENTS

I	INTRODUCTION	1
II	The SkelEx exoskeleton system	2
II-A	Kinematics of the system	2
II-B	Adjustment mechanisms	4
II-B.1	Amount of springs (Energy in system)	4
II-B.2	Length and thickness of springs (stiffness)	4
II-B.3	Spring material (stiffness)	4
II-B.4	Cable length (pre-tension)	4
II-B.5	Lever arm length (Moment arm)	4
II-B.6	Vertical spring constraint (restrict motion)	5
III	Design and requirements of the exoskeleton model	5
III-A	Modeling the leaf springs	5
III-B	Modeling total exoskeleton mechanism	6
III-C	Human Arm	6
III-D	Experimental setup	7
IV	Results	7
IV-A	Cable length adjustment	8
IV-B	Lever arm adjustment	8
IV-C	Vertical spring constraint	10
IV-D	Combination prediction	10
V	Discussion & Future Work	11
VI	Recommendations	12
VI-A	Method of force adjustment	12
VI-B	Spring clamping constraint	12
VI-C	Human arm constraint	12
VII	Conclusion	13
	References	13
	Appendix I: Flowchart of Research	14
	Appendix II: Spring setup	15
	Appendix III: Total model setup	17
	Appendix IV: ANSYS setup	19
	Appendix V: Additional figures	20

Modeling and altering the force profile of a spring-based upper body exoskeleton with design adjustments*

Ivo de Looij¹, Patrice Lambert², Gaurav Genani³ and David Abbink¹

Abstract—The SkelEx exoskeleton is a non-linear spring-based passive upper body exoskeleton that has the goal to compensate the weight of the wearer’s arms. Bending of three stacked non-linear springs transfers force from the hips of the wearer to the back of the upper arm. The amount of bending of the springs is a function of the geometry of the exoskeleton. The SkelEx exoskeleton was built using an iterative design method to evaluate all the length in the exoskeleton and tuned until the output force was balanced for a certain user. Now that this exoskeleton functions for certain user performing a certain task, the consequences of changing the geometry of the exoskeleton for a different users and applications is not known. The goal of this paper is to be able to predict the change in force curve when different geometric adjustments are made to the exoskeleton. The adjustments can be made into mechanisms that can be changed in the field of operation. The mechanisms that are reviewed are: the cable length, the lever arm length and the vertical position of a spring constraint. The force curve is defined as the amount of force that the exoskeleton provides at different arm rotations for in plane motion. Finite element models were developed in several steps, each of them supported by evaluation experiments in setups that were built for this purpose. The model is able to predict the force curve when the geometry of the exoskeleton is altered. The adjustment mechanisms can be used to smoothen the force curve and alter maximum output force.

I. INTRODUCTION

EXOSKELETONS are developed in various fields to aid humans. Exoskeletons that are used in industry and in the military aim to enhance the human capabilities such as strength or to reduce fatigue of the operator [1]. The military is developing exoskeletons with big rigid frames that empower the human so that they can lift heavy loads. An example of such an exoskeleton was developed by the University of California, U.C. Berkley, called BLEEX, which is a lower extremity exoskeleton designed to improve the strength of the legs so that the operator is able to carry heavy loads on his back [2]. The BLEEX system answered many key scientific questions, which were used by the company Berkeley Bionics to design the Human Universal Load Carrier called HULC: a lower extremity exoskeleton which could help carry the load in the backpack [3]. The

*This work was supported by SkelEx

¹Ivo de Looij and David Abbink are with the Biomechanical Engineering Department, Delft University of Technology, 2628CD Delft, The Netherlands

²Patrice Lambert is with the Precision and Microsystems Engineering Department, Delft University of Technology, 2628CD Delft, The Netherlands

³Gaurav Genani is the CEO of SkelEx, Yes!Delft Molengraaffsingel 12, 2629JD Delft, The Netherlands



Fig. 1: SkelEx Exoskeleton (December 2016)

results and performance are questioned in literature [4]. However, the HULC exoskeleton, and many other powered exoskeletons, did not provide a natural motion, making the exoskeleton exhausting to use. Furthermore, most of these enhancing exoskeletons are bulky, or are restrained in movement due to large power supply cables. Hugh Herr from MIT, states that the military focuses too much on big bulky exoskeletons, which, in his opinion, will not work for the near future because of the lack of understanding of the interaction between the exoskeleton and the human and available technology [4].

Untethered exoskeletons use batteries, fuel or compressed gases to store energy to operate. However, in almost every untethered exoskeleton the operating time is short and the added weight makes these exoskeletons impractical for use in the field. Power consumption is acknowledged to be the main limitation for this type of exoskeletons [5]–[11]. Therefore, strength enhancing, untethered exoskeletons are still in an early stage of development.

The actuator power-to-weight ratio is a big constraint in exoskeletons. Due to the weight of exoskeletons, higher torque actuators are necessary to operate the exoskeleton. Higher torque results in a higher power demand.

Until actuators are drastically improved, passive exoskeletons have the advantage when unrestrained movement for a longer period of time is necessary.

Since around 2010 the industry shows more and more interest in exoskeletons [12]. In industry, robotic technology is very common for a lot of applications, however due to limitations of these robotics, manual labor is still used for final assembly in for instance the automotive industry [13]. For these workers, heavy lifting in awkward positions is not uncommon. These workers face the risk of ergonomic in-

injuries on a daily basis. Ergonomic injuries or musculoskeletal disorders can have an affect on the muscles, nerves, skeleton, cartilage, ligaments and joints. These injuries occur due to for instance repetitive work or postural loads. Robotics are not yet viable to do these types of work due to the short task duration and limited mobility [13]. Research showed that 8.6% of the working population in the EU suffer from a work-related disease. 60% of the respondents that have work-related diseases state that their most serious work-related health problem are musculoskeletal problems [14].

Therefore exoskeletons are developed for industry to aid the workers [12]. The goal of these exoskeletons is to aid workers with heavy lifting or to decrease the muscle activity in a way that workers experience less fatigue and are less likely to sustain ergonomic injuries.

The difficulty with exoskeletons for able-body operators is that the acceptance of the exoskeletons is limited [12]. For the workers to use the suit, the benefits of the exoskeleton should greatly exceed the discomfort or decreased range of motion due to the exoskeleton.

A lot of professions are in need of an exoskeleton to help workers with overhead work, such as painters, workers underneath car lifts, plasterers or welders for example. For these types of jobs close-to-body exoskeletons are crucial. In for instance the shipyard industry, welders have to crawl through tight spaces and carry a welding machine. Moreover, the risk of collision with objects in the room decreases, when wearing an exoskeleton that is close to body compared to bulky exoskeletons. The operator does not have to consider the added body volume, which increases the maneuvering space of the operator. The risk of hitting something can have drastic consequences in industry as machines or products can be damaged. Therefore the exoskeleton needs to be as close to body as possible.

One of the exoskeletons that is developed for industrial use is the SkelEx exoskeleton (Figure 1). This exoskeleton is a non-linear spring based upper body exoskeleton that aims to relieve shoulder muscles when doing overhead work. This is achieved by compensating the weight of the wearer's arms. The working of this exoskeleton is explained in the next section.

This exoskeleton however, has the limitation that the force profile is fixed as the springs are loaded due to the geometry of the exoskeleton. Therefore, the force curve can not be altered to cope with different arm weights of the users or optimized for different applications. The exoskeleton has been tuned to a certain user until it functioned appropriately. However, for this exoskeleton, methods need to be found to alter the output force to cope with different users and different applications which again limits the acceptability. The force curve of this exoskeleton is also not yet predictable for the users. High forces are applied quickly on the arms creating a jerky motion. After the initial high force, the force is quickly decreasing. In order to change the force curve, the geometry of the exoskeleton needs to be altered. The geometry of the exoskeleton determines the loading conditions on the leaf springs that generate the force. Models of leaf springs have been built for the automotive industry

[15]. From these models it can already be learned that hysteresis in these type of mechanisms is present and the different models result in different stiffnesses depending on the assumptions of the model. The loading conditions on these leaf springs are however completely different, as out of plane bending occurs in this exoskeleton and the relative displacement is larger than for car leaf springs. Therefore, a finite element model is built to model the force curve that can be exerted by the exoskeleton.

A model of this system can be used to evaluate the critical parameters. The model needs to be more complex than a purely parametric model due to the fact the curve of the force is important. A pure parametric design, as a design tool, only supplies the maximum and minimal values as output parameters, and not the continuous shape of the force curve at different angles of the arm.

The model is validated using experimental data. With these validated parameter adjustments, a prediction of a combination of these parameters is made.

The goal of this paper is to be able to predict the way the force curve changes when exposed to different parameter variations and be able to alter the force curve with these parameters for different users and applications.

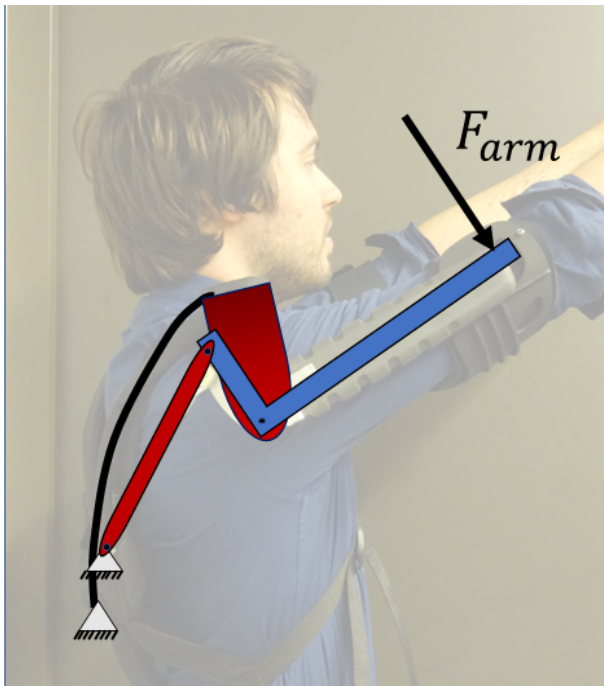
II. THE SKELEX EXOSKELETON SYSTEM

The SkelEx exoskeleton is a passive exoskeleton that aims to relieve shoulder muscles when doing overhead work. This is achieved by compensating the weight of the wearer's arms.

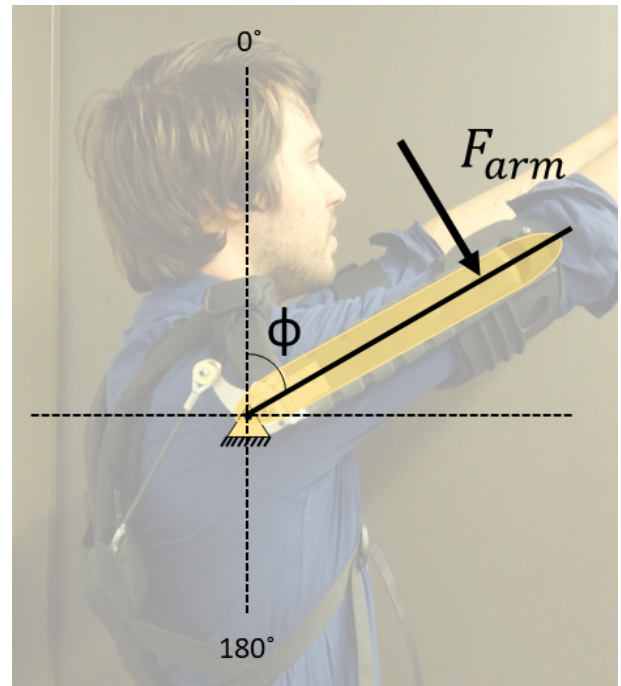
The elements that provide the force are stacked leaf springs. These leaf springs are attached to a frame which is mounted to the lower back. The force is transferred to the back of the upper arm to provide a lift force. This force should be smooth over the full range of motion and be zero when the arms are completely down, to make sure that the operator can comfortably stand without experiencing force when the operator doesn't need to lift his arms. These elastic elements provide the force, and also function as the structure of the exoskeleton. The exoskeleton consists of an elastic frame that has to fit several body types with different force requirements to cope with the different arm weights. The SkelEx exoskeleton was built using an iterative design method to evaluate all the points and tuned until it worked properly. Now that this functions for a certain user, the consequences of changing different geometric parameters are not known. To evaluate the system a simple 2D representation is further explained.

A. Kinematics of the system

The exoskeleton system can be seen as a double pendulum system, with two degrees of freedom, were the second link is shaped like an L-bar (Figure 3). The second link is also attached to the human arm. This arm can be simplified as a rotating beam that is the length of the upper arm (from shoulder joint to the attachment point of the exoskeleton to the arm, see figure 2b). The human arm now controls the angle of the L-bar link so that the system can be controlled by the angle of the human arm and the angle of the cable, so that



(a) 2D representation of Exoskeleton



(b) Force is measured on the arm with fixed shoulder joint. The angle (Φ) is 0 when the arms are raised

Fig. 2: Schematic of the SkelEx exoskeleton mechanism. The F_{arm} is modeled and measured at different angles of the arm (Φ) which defines the force curve

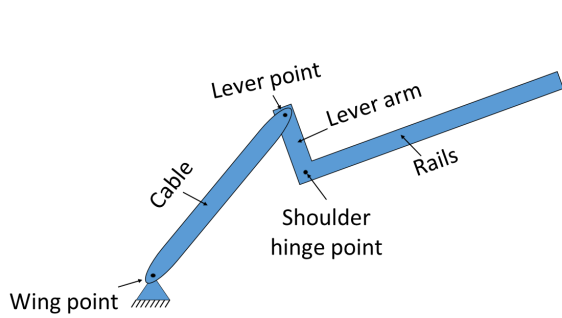


Fig. 3: Exoskeleton planar double pendulum representation. Used as a simple model to explain the working of the exoskeleton. The different names are shown that are used in this paper. The wing point is the position where the cable is attached to the frame. The shoulder hinge point is connected to the exoskeleton shoulder. This is the location where the spring force is applied. The cable can only exert a tension, therefore it can be modeled as a rigid link with two ball joints at either side.

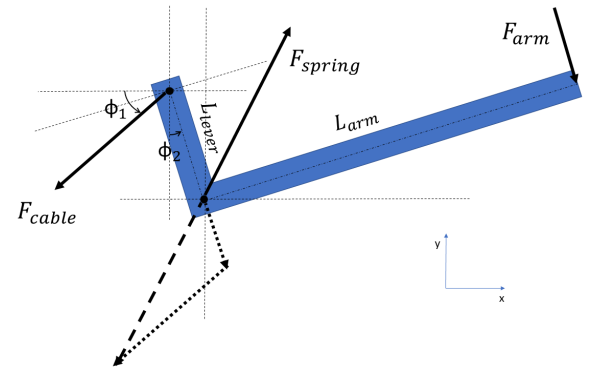


Fig. 4: The singularity point can be calculated with the F_{cable} , F_{spring} and the F_{arm} and the two angles that are defined for the double pendulum

it is still a two degrees of freedom system. The cable however is not actively controlled (Figure 5). The spring applies a force at the corner of the L-bar. The angle of the cable is therefore dictated by the minimum energy position of the spring. The human arm together with the energy in the spring can be seen as the two inputs to the system. The system is therefore not dictated to make a certain motion. If forces are applied at the system, the system will deflect in that direction.

The SkelEx exoskeleton configures the components in a

way that a mechanical singularity point is located at the position where the arms are down. This is the relaxed stance of the operator, which makes the SkelEx exoskeleton comfortable to use. No force is experienced when the operator moves the exoskeleton in its singularity point. The force on the arms of the operator increases when the operator raises their arms, because the effective lever arm increases (figure 4). The force of the spring decreases when the arms are lifted, due to the fact that the deflection of the spring decreases when the arms are raised. The output force is a relation between the effective lever arm and the amount of spring force. The singularity occurs when the L_{lever} aligns with the reactive force in the cable (figure 4 defines the naming of the forces and angles).

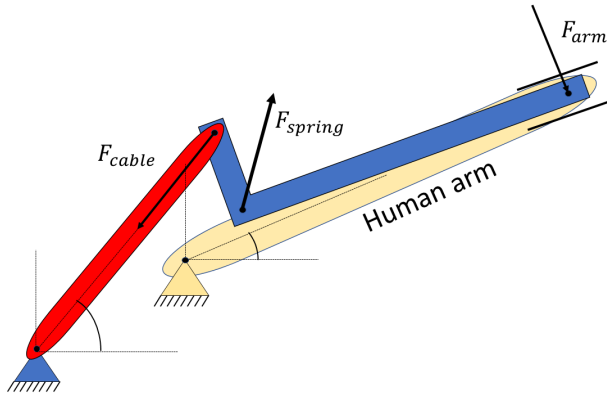


Fig. 5: Linkage of the exoskeleton to the human arm does not change the amount of degrees of freedom

This can be concluded from equations 1 to 4:

$$\sum F = 0$$

$$F_{spring} = F_{arm} + F_{cable} \quad (1)$$

$$\sum M = 0$$

$$F_{arm} \cdot L_{arm} - F_{cable} \cos(\phi_1 - \phi_2) \cdot L_{lever} = 0$$

$$F_{cable} = \frac{F_{arm} \cdot L_{arm}}{L_{lever} \cdot \cos(\phi_1 - \phi_2)} \quad (2)$$

Combining the two equations

$$F_{spring} = \left(1 + \frac{L_{arm}}{L_{lever} \cdot \cos(\phi_1 - \phi_2)} \right) F_{arm} \quad (3)$$

This equation increases to infinity when $\cos(\phi_1 - \phi_2) = 0$. This occurs when the F_{cable} and the lever arm are collinear. When solving for F_{arm} this transforms into:

$$F_{arm} = \frac{F_{spring} L_{lever} \cos(\phi_1 - \phi_2)}{L_{lever} \cos(\phi_1 - \phi_2) + L_{arm}} \quad (4)$$

So the structure reaches the singularity point when $|\phi_1 - \phi_2| = 90^\circ$.

The singularity point can be shifted by means of changing the angle between the L_{lever} and the L_{arm} . In this example the angle between the two is 90° . In order to get the singularity at the position where the arms are down the angle between these two links is increased. The angle of the lever arm can shift the phase of the force, however this also shifts the singularity location. In the singularity position of the system the operator can comfortably stand without experiencing force when the operator doesn't need to lift his arms. From previous investigation it has been noticed that shifting the singularity position to another location is experienced as very uncomfortable. Therefore, changing the angle of the lever arm is not further considered in this paper.

This system, however, is still very much a simplification of the actual system. The actual system can have out of plane motion. The fixation point of the spring and the fixation point of the cable (wing point) are not in one plane. This

exerts an additional torque on the springs creating out of plane bending. The springs will have out of plane bending, bending away from the shoulders. The F_{spring} is therefore also in 3D. This alters the amount of force that is exerted on the arms. The principle of the equations 1-4 still hold. The cable can only exert a tension, therefore it can be modeled as a rigid link with two ball joints at either side. The ball joints are necessary to cope with the out of plane bending of the spring. Moreover, an additional joint is added between the shoulder hinge joint and the rails to cope with this out of plane motion. This additional joint increases the range of motion of the exoskeleton as the arms can now move in the horizontal plane. If the system works properly, the attachment of the exoskeleton arm to the human arm provides interaction between the exoskeleton and the operator as well as the attachment of the frame to the lower back. If the fit is incorrect, the springs can hit the user which provides another interaction location with the exoskeleton. This collision with the user is undesired and therefore the interactions at places other than the intended location, are not further considered. Now that the working of the exoskeleton system is explained, methods to alter the output force of this exoskeleton system are investigated in the next section.

B. Adjustment mechanisms

There are multiple parameters that can change the force in the system. Some of these parameters are more suitable as an adjustment mechanism than others.

1) *Amount of springs (Energy in system)*: adding a higher number of springs will increase the amount of energy in the system. These springs are stacked in parallel so adding another spring will drastically increase the force. Therefore, this is not feasible as a delicate adjustment method.

2) *Length and thickness of springs (stiffness)*: the spring length, is a function of the anthropomorphic dimensions. A bigger person requires a higher output force because of the weight of the arms. However, because of the user's volume the spring needs to be longer decreasing the output force which is counter productive. Altering the thickness of the springs will drastically increase the force however the stresses in the material are higher which will result in plastic deformation faster.

3) *Spring material (stiffness)*: altering the spring material is a solution to change the stiffness and the behavior of the springs, however, this completely changes the response of the system. Also, the spring material can not be changed in the field.

4) *Cable length (pre-tension)*: the cable length dictates the distance between the lever arm (lever point, fig 3) and a fixed point on the exoskeleton (wing point), loading the spring and creating the preload. The spring is tensioned more as the length of the cable decreases, increasing the force of the spring.

5) *Lever arm length (Moment arm)*: the length of the lever arm determines the length of the moment arm over which the force is applied on the arm. Also in singularity, the shoulder hinge point is moved closer to the wing point

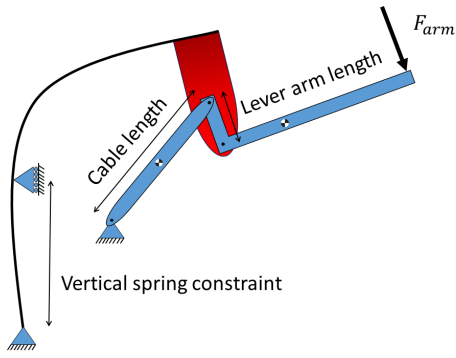


Fig. 6: Parameters that can alter the force with small increments, that can be changed in the field

as the distance is then equal to the length of the cable minus the length of the lever arm, storing a larger amount of energy in the system.

6) *Vertical spring constraint (restrict motion)*: the vertical spring constraint restricts the free motion of the spring. Therefore, the amount of energy that the spring contains can not be released all at once as the spring can not change shape as quickly due to this restriction. An added benefit of the vertical spring constraint is that it prevents the spring from moving too far to the front, colliding with the operator.

Parameters such as the amount of springs spring length and thickness, spring material, can all alter the output force. However, a more subtle force adjustment system is required. Therefore these solutions will not be further examined for now. There are three adjustment features that are tested in this paper, that can affect the force curve of the exoskeleton. These parameters can be easily changed in the field of application without the need of tools. The parameters that will be examined are also graphically represented in figure 6 and are the cable length, the lever arm length and the vertical spring constraint.

A lot of mechanisms exist to increase or decrease the distance between two points. Therefore an easy solution can be found to apply these changes to the system.

In order to be able to predict the response of the system, a model has to be made. The model should be able to capture the force curve of the real system, so that the positive and negative effects can be examined and the force adjustment mechanisms that can alter the height and smoothness of the force curve can be implemented.

III. DESIGN AND REQUIREMENTS OF THE EXOSKELETON MODEL

The aim of this model is to be able to see the difference in force curve by changing parameters on the exoskeleton design. The design of the exoskeleton is not altered as this design is the trademark of the company. However, adjustment mechanisms and lengths of these parameters can be altered in this study. In this way the contribution of this work is to be able to customize the force curve of this exoskeleton in a way that different weight of arms can be supported by the

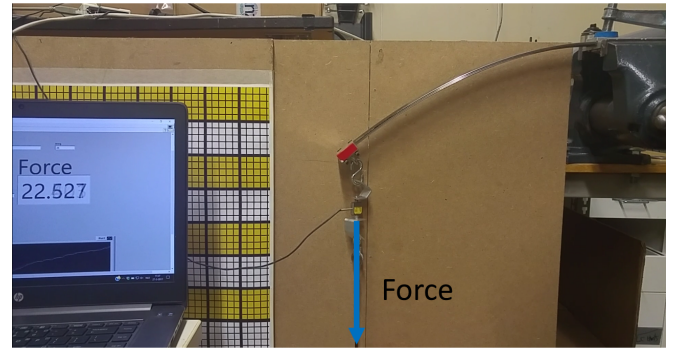


Fig. 7: Leaf spring measurement setup

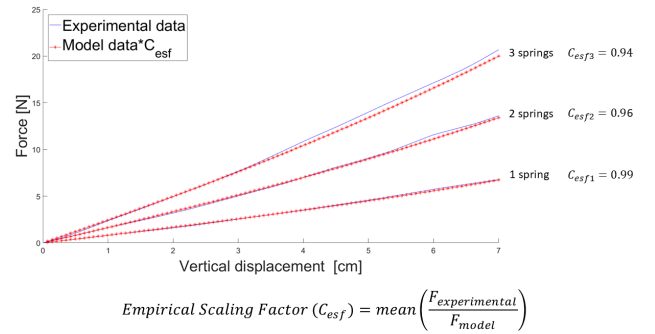


Fig. 8: Adjusted spring force resulting from tip displacement. A comparison between the ANSYS data and the experimental data

exoskeleton without compromising beneficial effects to other parts of the exoskeleton.

A. Modeling the leaf springs

The SkelEx exoskeleton stores the energy into leaf springs that are mounted on a frame which is attached to the back of the operator. The leaf springs are stacked on top of each other and clamped at both ends. The leaf springs are the elastic elements that provide the balancing force for the arms. Therefore, in order to create a model of the total system, the behavior of the springs was examined first. The geometry and material properties of the springs were examined so that the spring force-deflection curves were accurate (figure 7).

The friction, amount of substeps and mesh size were examined. From this study, it was concluded that all these factors have influence on the exact value of the force, however the shape of the force is not influenced by these factors. Instead of increasing the computation time it was decided to remove friction between the springs as the effect was minimal. The amount of substeps and mesh size were chosen to give the right force curve and least amount of computation time, as the force curve is the most important factor. An empirical constant was used to create the same force curve for the ANSYS model as the one that was measured with the experimental setup (figure 8). This reduced the computation time significantly and yielded the same force curve as the experimental setup.

Constraining the springs in the same way as the actual

exoskeleton system is challenging as little is known about the behavior of the clamping mechanism. If the ANSYS model is constrained so that the springs have to follow a path which is not the path of least energy, the output force on the arms drastically increases. This is because the spring can then try to elongate or buckle. This is not the natural behavior of the spring and therefore not the correct way of loading the system. The pre bend of the springs increase the interaction complexity between the springs when the leaf springs are stacked. If the stacked leaf springs are bend, the radius over which the springs bend is different. Because of this difference, the springs must be able to slide on top of each other. Moreover, the clamping can create internal forces in the model that do not exist in the experimental setup. Therefore instead of applying an unknown clamping force at the tip of the springs, a no separation constraint was applied. This constraint bonds the nodes together in the normal direction, however it allows for sliding of the surfaces. The data of the experimental setup was collected using video tracking software (Kinovea). With this tracking software the deflection was measured. The amount of vertical deflection could be linked to the reaction force of the spring. With the single spring the geometry and material properties were validated and then multiple springs were added. After the simple spring setup was created, the model constraints were validated to create a similar response to the input. An empirical constant was necessary to scale the model data to the experimental data that was better than 10% (figure 8).

B. Modeling total exoskeleton mechanism

After validating that the model could describe the correct force curve for the amount of deflection, the movement of the spring tip could be implemented. The force provided by the springs could be calculated when the amount of deflection is known. The path described by the springs however, was not known. Therefore, the total system was implemented as well, such that the different paths could be modeled. The path that the spring travels depends on the geometry of the model. The initial exoskeleton was measured and implemented to create a benchmark of the system.

The cable length in the exoskeleton pretensions the system, which creates an initial bending of the springs. In the ANSYS model, a cable was implemented with a longer initial length and then shortened to the actual length to create the right preload in the system. Implementing the cable in this way also gives the benefit that the cable length could be easily altered as it was implemented as a cylindrical joint displacement.

The same was done for the lever arm. The lever arm was implemented as a translational joint in this way the lever arm could be altered to different lengths. All the joints in the model were modeled as undeformable joints.

The vertical spring constraint was implemented as a zero displacement constraint in x-direction, where the x-direction is defined as the perpendicular direction to the frontal plane. This zero displacement was applied at the vertex closest to the median plane, as this vertex is the one that is touching

the constraint without restricting the torsion that is applied on the springs. These changes were all conducted in the first loading step where the "human" arm link remained in the vertical position.

Furthermore, in the total exoskeleton model, the springs had interaction contacts with the shoulder part; therefore, the shoulder part and the springs were both implemented as a flexible parts. All the other elements in the system are modeled as rigid after examining the effect. The model without rigid components gave no significant difference in force curve however the computation time more than tripled.

The interaction of the springs with the shoulder part as well as each other was implemented as follows: the springs were in frictionless contact with each other as well as with the shoulder. At the bottom of the springs a fixed constraint was implemented. At the top part of the springs, no separation constraint was implemented to keep the springs together as they do in the clamp. However, in this system instead of a clamping force it is assumed that the springs can slide as the radius of the springs differ. In order to achieve this, the inside spring, the spring closest to the human body, is bonded with the shoulder part. This means that no movement between this spring and the shoulder is allowed. This was done to constrain the other springs from separating without restricting the sliding.

C. Human Arm

The ANSYS model requires a loading condition that is comparable to the input of the human arm. The human arm is connected to the exoskeleton by placing the arm in an arm cup. The arm is then fixed to the arm cup with Velcro strap. This, however, is not a viable constraint to model. Instead of implementing a human arm a torque on the shoulder joint of the exoskeleton could be implemented. However, this results in a loading condition that is not representable with loading that is applied by the human arm. The force that is applied on the exoskeleton arm results in bending of the spring and not necessarily in rotation of the arm. Applying a torque instead of a force results in a different motion. Therefore, a simple model of the human arm was built. The human upper arm, where the exoskeleton is attached, is modeled as a rotating beam that is connected at the shoulder with a revolute joint providing an in-plane rotating movement.

This connection between the human arm and the exoskeleton arm is modeled as a joint with three rotations perpendicular to each other. This is because the arm can slide and rotate a bit inside the arm cup due to the Velcro constraint, which does not do anything except for giving a secure feeling and preventing the arm from accidentally slipping out the cup.

Sliding is already implemented inside the exoskeleton arm with a linear guiding rail. The linear guiding rail is necessary to cope with the out of plane movement of the arms, as well as with the shoulder misalignment when the arms are raised. Furthermore, when the springs are loaded, out of plane motion occurs of the exoskeleton's shoulder hinge. Therefore, the relative length between the exoskeleton

shoulder hinge and the arm attachment changes making the slider indispensable.

The rotations in the arm cup are implemented in the model so that the model arm could be attached to the exoskeleton system. All these degrees of freedom in the connection between the human arm and the exoskeleton arm are necessary because of the misalignment between the human shoulder joint and the exoskeleton shoulder joint. Misalignment in joints needs to be minimized as this can lead to injury and strain to the joints of the operator. This is however minimized due to the exoskeleton's design. The springs release energy when the arms are raised, moving the shoulder joint of the exoskeleton upwards. When a human raises his arms, the shoulders rise as well minimizing the misalignment with the exoskeleton joint [16].

D. Experimental setup

The experimental setup was created in the same way that the model was developed. An arm was built that was the input to the system. Extracting consistent data without the input arm is very challenging as the flexibility of the system and the upper arm hinge movement need to be dictated very strictly. If the force is measured at the end of the exoskeleton arm, the end needs to be controlled properly. When the shoulder hinge can rotate freely, the spring can release its energy quickly by moving in the opposite direction of the end of the exoskeleton arm. This can be compared with balancing an inverted pendulum. Therefore the input arm was used to properly constrain the movement so that the movement can be dictated in the same way as it is when the operator is wearing the exoskeleton.

However, in comparison with the model, the revolute joint that represents the human shoulder was shifted to the side. This was done to eliminate the possibility of collision between the input arm and the exoskeleton system. If the leaf springs are loaded more, the springs deflect more. This large deflection will be stopped by interaction with the human. However, the exoskeleton is not supposed to have this kind of interaction with the human body as this creates pressure points leading to discomfort for the user. In order to be able to test the device without interference of the human, the shoulder was shifted to avoid collision. The input arm was mounted with roller bearings to the frame. The friction had to be minimized to reduce the hysteresis loop in the measurements. The axis of the arm is attached to a potential meter to measure the angle of the input arm. At the end of the arm a load cell is attached to measure the force perpendicular to the arm. Measurements on this experimental setup were compared to the ANSYS model to validate the response of the model to the different mechanism adjustments.

IV. RESULTS

Now that the working of the model is demonstrated, methods of force manipulation were tested. Humans have different proportions and different preferences. The spring needs to bend over the shoulder of the worker, however the size of this person varies significantly. Shoulder pressure will

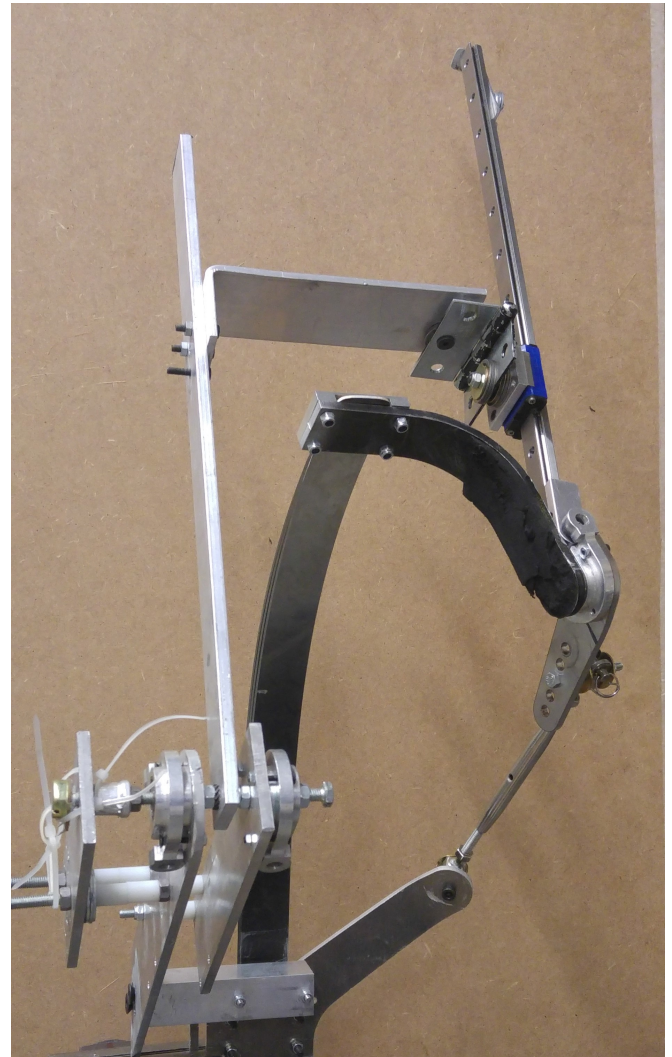


Fig. 9: Experimental setup

occur due to improper fitting of the exoskeleton. Not only the size of the users differs, also the weight of the arms of the wearer varies, creating demand for an adjustable force amplitude so that the arms feel weightless for every wearer. Different methods can be found to change the force, however the consequences for each method with respect to practicality and positive and negative side effects result in feasible and less feasible adjustment mechanisms. The figures in this section show the force as a function of the rotation of the arms. The arm angles range from 0 to 180 degrees in these measurements (figure 2). This is done because the exoskeleton operates in the frontal plane. The zero degrees angle represents the location where the arms are straight up. This is the location where the arms start loading the system. The position around 180 degrees is the position where the mechanism reaches its singularity. This is the position where the arms are relaxed and positioned down next to your body. In the model the arms rotate towards an angle of 190 degrees to make sure that the location of the singularity point is documented even if it has passed the ideal position of 180 degrees. The exoskeleton is mechanically constrained so that

is does not surpass this singularity point. If the cable was able to cross this singularity point, the force on the arms would reverse, pulling the arms backwards. In this way the exoskeleton can only exert a force on the arms resulting in a motion in front of the operator.

The force curve from the model is collected together with the experimental data so that it was possible to compare both force curves respect to the adjustment mechanisms. Two sensors were used in order to collect the data from the experimental setup. A potentiometer (B10K Linear potentiometer) was used to track the angle of the input arm and a load cell (MODEL FLLSB200 S-BEAM Junior Loadcell) was used to measure the force perpendicular to the input arm at location where the cup is attached to the arm.

A. Cable length adjustment

One of the solutions to create a different force curve was by altering the length of the cable. The cable length alters the distance between the lever arm and the wing point on the frame, thereby loading the spring and creating the preload. This tension however also lowers the amount of volume that the spring encloses. The end point of the spring is closer to the body when the cable is shortened which can result in a contact point between the spring and the shoulder.

Figure 10 shows that indeed by shortening the cable the total force increases. The outcome of the model was checked to see if the model responded the same way to the adjustments as the real system does. The experimental data is compared with the ANSYS data in figure 10 for the different cable lengths. The model data showed that the cable length changes the force and the location of the maximum. This analysis is confirmed with the experimental data.

The experimental data shows a hysteresis loop which is due to the friction in the exoskeleton system (figure 10, right). Moving the arms down, which is the movement to load the springs, requires more force than the opposite movement when the system releases its energy, on the arms of the operator. The two lines in the experimental data with the same color represent the down and up movement of the arm.

Friction is not implemented in the ANSYS model therefore the up and down movement would result in the same amount of force applied on the arm. Nonetheless, the experimental data shows the same response due to the adjustment feature as the ANSYS data.

The experimental data also shows that the higher output force of the exoskeleton also increases the amount of hysteresis in the system. More force on the system means higher friction components as well.

The maximum force is located at the position where the arms are turned further down when the cable length is decreasing. Also noticed is that the force shape remains the same at lower angles and is only shifted further up. The same response was measured with the experimental set-up.

This slight shift in the location of the force maximum also affects the singularity point, however this is only a difference of $\sim 2.5^\circ$ in arm position. This variation in singularity position can however not be measured accurately enough to confirm this shift with the experimental setup.

The small variation in maximum location is due to the fact that the angle of the cable is differing. The hinge point is closer to the wing point for a shorter cable length. For shorter cable lengths this results in a faster jump in force when the arms are almost down. This results in a jerky motion when the arms are moved up again. Overestimated or underestimated force on the body results in over- and undershoot when aiming for a desired target [17]. This unwanted effect, of the sudden increase of the force, should be taken into account when trying to increase the force with this method.

The data shows that for a longer cable length the sudden jump in motion reduces, however the force that is then applied on the arms is not enough to give the wearer the amount of support to compensate the weight of the arms.

From this data it can be seen that the amount of change in force is not very high when altering the cable length.

The trend line that is obtained using the ANSYS data is also depicted on top of the experimental data. The trend line of the ANSYS data is shifted down with 20N in order to align with the experimental data

The cable length between a range of $\pm 20mm$ around the original cable length can be linked to the maximum peak force ($Cable_{Force,max}$) and the angle on which this peak force occurs ($Cable_{Angle,max}$). The formulas for this ANSYS trend line for a cable length variation as input (c_l [-20 20]) are equal to:

$$Cable_{max,Angle} = -0.0012c_l^2 + 0.4308c_l + 147.7100 \quad (5)$$

$$Cable_{max,Force} = 0.0009c_l^2 + 0.4028c_l + 45.5057 \quad (6)$$

These formulas can predict the location and amplitude of the maximum force when the cable length is altered. The original length is implemented as an cable length variation of 0.

B. Lever arm adjustment

The lever arm length is next adjustment that can alter the amount of force that can be created by the springs.

The lever arm rotates around the shoulder hinge while tensioning the springs. The longer lever arm drastically increases the output force of the exoskeleton. The springs are bending more because the shoulder hinge is located closer to the wing hinge in the singularity point increasing the total amount of energy in the system. This stored energy is quickly released when the moment arm is slightly increased, due to the angular rotation of the human arm. This occurs due to the sinusoidal behavior of the lever arm. This quick release in energy results in a sudden increase in force on the arm, making it hard to move the arms in a smooth manner. Unexpected movements result in overshoot and co-contraction. It has been well known that co-contraction requires more energy and muscle activity. The exoskeleton suit wants to decrease muscle activity, and reduce fatigue. Therefore shifting the maximum force peak to the right is unwanted. It can be seen that the first 90 degrees are a lot more stable which is the workspace of the arms straight

Model validation of cable length adjustment

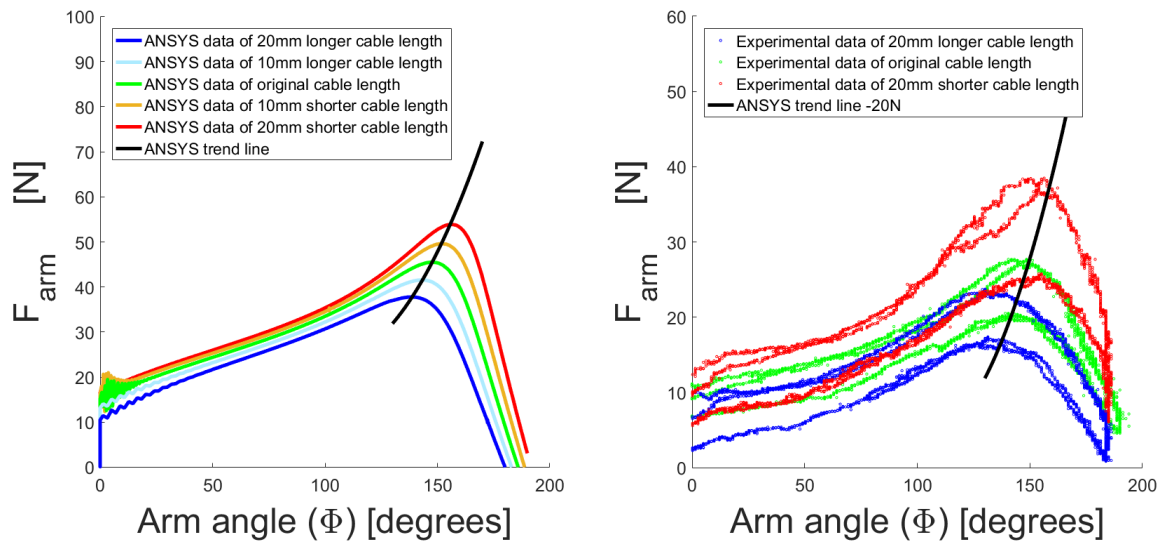


Fig. 10: second order trend lines for cable length adjustments. The blue, green and red lines are used to evaluate the trend line. The two other lines are evaluated and follow the trend line. In the experimental data the two lines with the same color represent the down and up movement of the arms, the difference between the lines is the amount of hysteresis in the system

Model validation of lever arm length adjustment

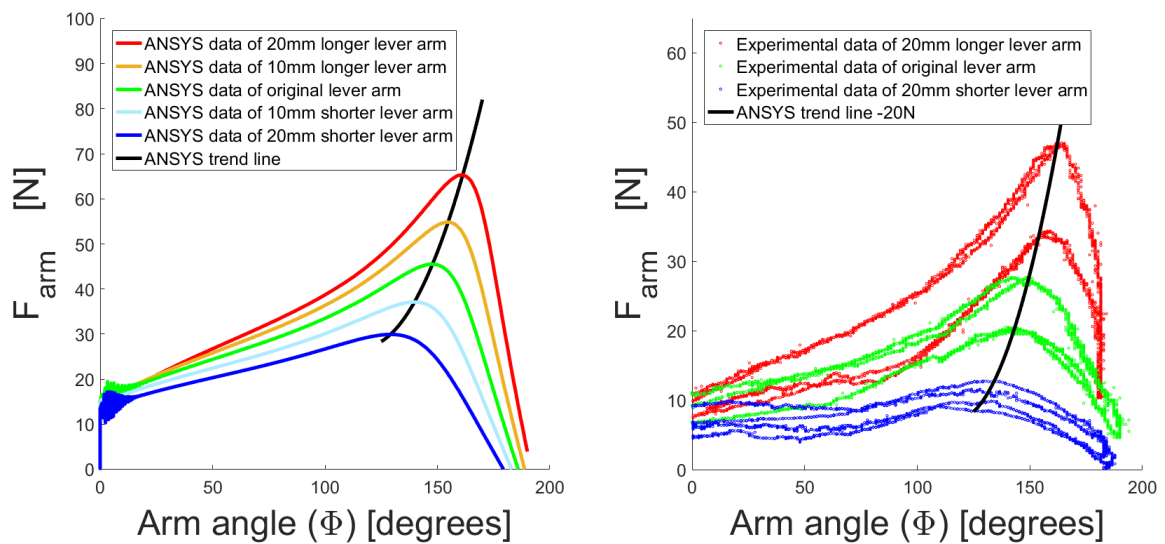


Fig. 11: second order trend lines for lever arm length adjustments. The blue, green and red lines are used to evaluate the trend. The two other lines are evaluated and follow the trend. In the experimental data the two lines with the same color represent the down and up movement of the arms, the difference between the lines is the amount of hysteresis in the system

forward to above the head. This is the area for which the product is designed. However, in order to operate the suit in a predictable manner, the energy should be released more gradually.

The trend line of the ANSYS data that shows the height and location of the maximum force can be expressed as a second order function.

The lever arm length, between again a range of $\pm 20mm$ around the original lever arm length, can be linked to the maximum peak force ($La_{Force,max}$) and the angle on which this peak force occurs ($La_{Angle,max}$). The formulas for these trend lines with lever arm length variation as input (l_i [-20 20]) are equal to:

$$La_{max,Angle} = -0.0064l_i^2 + 0.8055l_i + 147.7100 \quad (7)$$

$$La_{max,Force} = 0.0052l_i^2 + 0.8839l_i + 45.5057 \quad (8)$$

With these formulas the location and the amount of force can be predicted with different lengths of the lever arm. The trend line of the ANSYS data is shifted down 20N to align with the experimental data.

C. Vertical spring constraint

The last adjustment type that is going to be evaluated is the vertical spring constraint. This constraint is a stop located at a certain vertical distance from the spring base. This stop constrains the spring at a point so that that point is unable to move in horizontal direction. This point is not constrained in all other directions allowing it to move when the spring is bending out of plane. The maximum peak value of the force is decreased as the spring is not able to bend as far as before. It also limits the movement of the spring so that it benefits the fit of the exoskeleton. A large deflection of the spring will result in collision with the operator. The pressure of the spring on the shoulders of the user will be removed because of this vertical constraint.

The ANSYS model of the exoskeleton system with the vertical spring constraint shows a smoother force profile in the region of 90 degrees to 180 degrees (Figure 12). The unrestricted spring is allowed to move in the direction it wants, creating a jump in force. The constrained spring is not able to release all its energy at once, giving a slower increase in force. The force has a more flat response over the full range of motion making it more predicable to use. From figure 12 it can be seen that the vertical spring constraint brings down the peak force but increases the force when the arms are raised, increasing the support to the operators as they have to work above their head.

Figure 12 also shows the experimental data for two different systems, the original system in green and the system with a vertical spring constraint at 150mm from the spring attachment point in orange. It can be seen that the force jump is removed, and the force remains constant for a large range. Also, the experimental data shows that indeed the force on the arms is higher when arms are moved in the upright position when the vertical spring constraint is implemented.

The original system increases the force quicker when the arms are moved upwards than the system were the vertical spring constraint is present.

The vertical spring constraint also changes the offset of the maximum force on the arms. The maximum force is shifted to a location where the arms are positioned higher. The location is shifted because the bending radius decreases, so the hinge point can't reach the original position, increasing the angle of the cable. This is however less noticeable because the force peak is wider, giving a more uniform force profile. It can be seen that with this vertical spring constraint there exists a invariant point. A circle can be created from this invariant point that shows that the left side of this point is raised when the vertical spring constraint is increased and the right side is decreased. This circle shows the behavior of these vertical spring constraints however, it is not considered to be a quantitative trend line as only one point on the circle is defined which is the peak of the system without a vertical spring constraint (green, figure 12). Therefore, the circle only a visualization of the shift in the location of the force. This plot however, shows that with this constraint the force curve can be made more smooth. Decreasing the peak force at $90^\circ - 180^\circ$ is experienced as a smoother force curve.

The trend lines are able to predict the location of the intermediate lines, so that a continuous predictions can be made with different input values for the adjustment mechanisms. However, the influence of the adjustment mechanisms on each other needs to be further examined.

D. Combination prediction

Adjusting the lever arm results in a large increase in maximum force, however some negative effects are present. The lever arm is a rotating part, increasing its length can add the risk of hitting the surrounding with the suit. Also, the sudden increase in force has negative effects on the controllability of the suit. However, it has been seen that the vertical spring constraint is able to reduce the peak force at the $100^\circ - 180^\circ$ range. A combination of the different adjustment systems can be a solution to create a higher output force without creating a jerky motion.

Figure 13 shows that indeed the effects of both adjustments can be combined. The long lever arm was combined with the high vertical spring constraint. This combination can provide a higher force which is suitable for people with heavier arms. The higher force due to the longer lever arm was combined with the vertical spring constraint to flatten the ramp of the force while increasing the total force. The increased amount of force that was created by the longer lever arm is released in a controlled manner distributing the force more evenly over the total range of motion. The amount of force at the different locations can be controlled by increasing or decreasing the vertical spring constraint as this shifts the amount of force from the location where the arms are in the lower 90 degrees to the location where the arms are further raised. With the use of these adjustment mechanism a higher or lower force can be obtained and the smoothness of the curve can be altered.

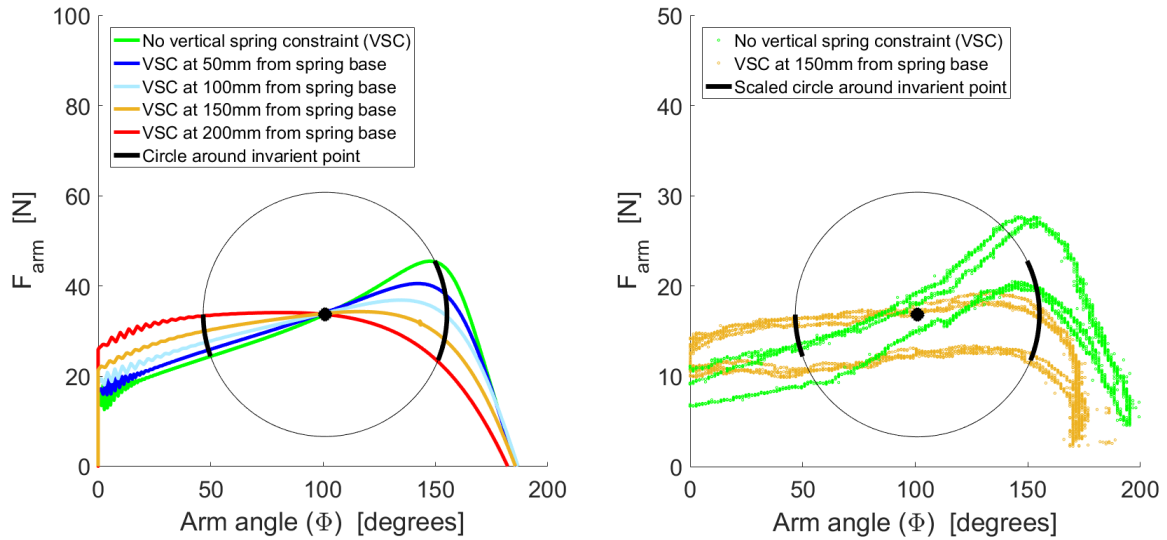


Fig. 12: Vertical spring constraint adjustments with circle through invariant point that shows the decrease in force on the right side from the center and an increase in force on the left side from the center. In the experimental data the two lines with the same color represent the down and up movement of the arms, the difference between the lines is the amount of hysteresis in the system

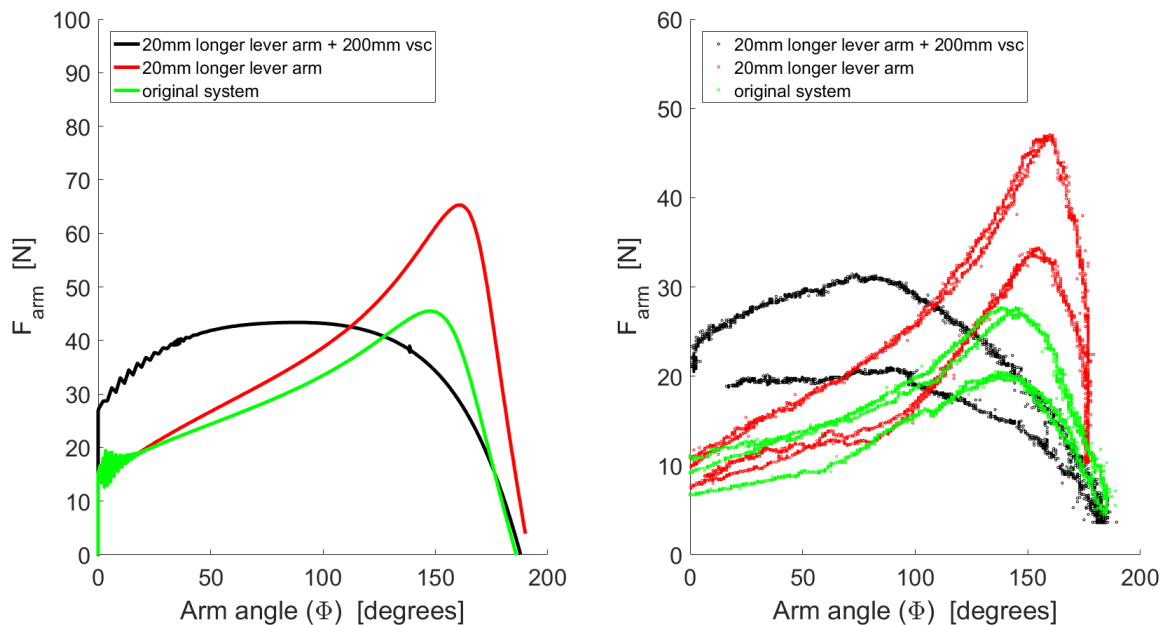


Fig. 13: Combination of different adjustment mechanisms, the force could be adjusted to give a flatter and smoother response with the vertical spring constraint and the height of this force can be altered with the lever arm

V. DISCUSSION & FUTURE WORK

This research was conducted in order to evaluate geometric parameters that could alter the behavior and the amount of force so that adjustment mechanisms could be developed. This behavior of the force curve is captured in this research and adjustment mechanisms can be developed accordingly. The model that was built for this purpose has however some limitations.

In this model, the gravity component was not added. This was done because the current model only considered changes in length with newly added adjustment mechanisms in the model. The weight of the components of the experimental setup and the ANSYS model is therefore not the same.

In the ANSYS model a gravity component could be subtracted which was already tested by implementing a point mass at the end of the human arm input link. This created a more curved line which looked closer to the experimental

data however, for this model to be more accurate the weight of all the components should be taken into account. This can be done in the next version of this model. However, even though the shape changes a bit, the trend lines remain similar.

Furthermore, no friction was assumed in this model; this was done because current constraints in the exoskeleton are not final yet. The way that the springs are constrained is not the right way as it is done with clamping, however sliding is allowed. Also in order to obtain the complete hysteresis loop in the ANSYS model the motion should be done twice, once from 0 to 180 degrees and then back to 0 degrees. This would double the computational time without adding a lot of new information about the exoskeleton system.

The trend lines of the ANSYS simulation are now plotted over the experimental data to show that the trend of the experimental data follows the same line as the ANSYS data. In order to compare the trend lines of both the experimental data and the ANSYS data, more experimental data needs to be obtained. With more data, the average of the experimental data can be obtained so that the trend lines can be statistically compared. In this research, the trend line of the ANSYS data was plotted on top of the experimental data and shifted down. This method showed already that the data compares well as the peaks of the experimental data followed the trend line of the ANSYS data.

The ANSYS data could be used to predict the behavior in a qualitative fashion. The exact values extracted from ANSYS are not the same as the experimental values. However, the force curve describes the same path, the ANSYS data can be scaled to the experimental values. This requires an empirical scaling factor in order to predict the exact value. Until the exoskeleton system is improved so that the amount of hysteresis is reduced, using a scaling factor is enough to predict the output force.

The trend lines could be described quantitatively for the cable length variation as well as the lever arm adjustment. The vertical spring constraint shows an invariant point. This point could be shifted towards a location were the arms are raised further when the lever arm increased. Trend lines for combinations of adjustment mechanisms need to be further examined.

VI. RECOMMENDATIONS

A. Method of force adjustment

As shown in the Results section, both the cable length as well as the lever arm are able to adjust the force of the exoskeleton suit. However, the most effective way of adjusting the force is by creating a different length lever arm. The downside of both adjustment systems, and especially the lever arm, are the fact that the force increases more rapidly when the energy in the system is higher. Therefore, the vertical spring constraint is a method of decreasing the rapid release in energy, which results in a less jerky motion. The recommendation is to add the vertical spring constraint to the system and adjust the amount of force using a lever arm adjustment. In that way the force curve remains smooth,

and the amount of energy in the springs can be varied. The higher the vertical spring constraint the higher the force is that is pressing on this constraint.

A rapid increase in force provided by the exoskeleton creates a larger δF which is the difference between the lifting force and the gravity force that is applied on the arms. Ideally this should be zero. The larger this difference, the less smooth or more jumpy the force feels on the operators arms as this δF results in an acceleration of the arms.

Moreover, due to this vertical spring constraint, the shoulder hinge point is not moving as far to the front as before. This can result in more misalignment with the shoulder joint. Therefore, because more misalignment is present, a longer rails on the arms are needed to cope with the shift in shoulder joint. An optimum needs to be found as a function of the geometry of the human body. If the rails are too short, the force on the vertical spring constraint increases significantly pushing the frame against the human body. This creates an uncomfortable pressure against the back.

B. Spring clamping constraint

The method that is now used to attach the springs to the frame and the shoulder piece is done with a clamping block. This clamping block restricts the springs from moving apart. However, sliding of the springs is necessary because of the difference in radius. Therefore, this clamping mechanism restricts the possibility for springs to slide properly, adding significant friction and uncertainty to the system. The amount of clamping has effect on the amount of output force which is undesirable as this makes every exoskeleton slightly different. Properly constraining all the elements makes the system more predictable and consistent. Furthermore, some of the rotation points in the system are not yet mounted with plain or roller bearings. Improving these joints can reduce the amount of friction that is present in the system. Decreasing the amount of friction will reduce the hysteresis loop that is present in the exoskeleton.

C. Human arm constraint

The arm of the human is attached to the exoskeleton arm. This attachment needs three rotations as there is always misalignment of the exoskeleton shoulder with the human shoulder. The exoskeleton shoulder is more laterally located than the human shoulder which creates an angle between the human arm and the exoskeleton arm, which means that the exoskeleton arm rotates on another plane than the human arm. To account for this misalignment more degrees of freedom shoulder be added to the arm cup. The cup with the Velcro accounts for a lot of those necessary degrees of freedom however, this might be a study to increase comfort. The arms do not have to move as much within the arm cup, as they are have to at the moment. This movement of the arm inside the cup creates a rubbing sensation of the fabric on the skin which may be experienced as unpleasant.

VII. CONCLUSION

In this paper, the force curve adjustment methods of the SkelEx exoskeleton are described. This exoskeleton is a new exoskeleton that is designed to aid workers to assist the arms when doing work in front or above the head. The novelty of this exoskeleton is the way that it generates its force. The force output is created by loading stacked leaf springs, which makes the exoskeleton flexible and more intuitive to use. Methods were needed to adjust the force curve that this exoskeleton could generate. This is desired in order to provide different kinds of force profiles for different applications and different users with this exoskeleton. In order to do that, different geometric parameters were altered to change the force curve. These parameters were the cable length, the lever arm and the height of the vertical spring constraint. A finite element model was developed that could describe the shape of the force curve when these parameters were altered. A second order trend line could describe the locations of the maximum force for the adjusted cable length as well as for the adjusted lever arm length. The vertical spring constraint showed interesting response with an invariant point, however this could not be described with a trend line. It was able to shift the maximum force, but not able to increase the maximum force.

It was found that with those validated adjustment mechanisms it was not possible to create a high and smooth force curve with a single adjustment mechanism. The model was then used to combine two adjustment mechanisms. With the combination of the lever arm length and the vertical spring constraint it could be seen that the output force could indeed be altered to a higher and smoother force curve. This prediction was then validated with the results from the experimental setup. And therefore, it can be concluded that indeed by combining two mechanisms, the force curve can be transformed into a higher and smoother force curve. Also this model can predict the behavior of the force curve when different geometric alterations are applied.

REFERENCES

- [1] C. Kopp, "Exoskeletons for warriors of the future," *Defence Today*, vol. September, pp. 38–40, 2011.
- [2] A. B. Zoss, H. Kazerooni, and A. Chu, "Biomechanical Design of the Berkeley Lower Extremity Exoskeleton (BLEEX)," *IEEE/ASME Transactions on Mechatronics*, vol. 11, no. 2, pp. 128–138, 2006.
- [3] R. Bogue, "Exoskeletons and robotic prosthetics: a review of recent developments," *Industrial Robot: An International Journal*, vol. 36, no. 5, pp. 421–427, 2009. [Online]. Available: <http://www.emeraldinsight.com/doi/abs/10.1108/01439910910980141>
- [4] W. Cornwall, "In pursuit of the perfect power suit," *Science*, vol. 350, no. 6258, pp. 270 LP – 273, 10 2015. [Online]. Available: <http://science.sciencemag.org/content/350/6258/270.abstract>
- [5] H. Kazerooni, "Exoskeletons for Human Power Augmentation," vol. 3120-3125., pp. 3120–3125, 2005.
- [6] H. S. Lo and S. Q. Xie, "Exoskeleton robots for upper-limb rehabilitation: State of the art and future prospects," *Medical Engineering & Physics*, vol. 34, no. 3, pp. 261–268, 2012. [Online]. Available: <http://linkinghub.elsevier.com/retrieve/pii/S1350453311002694>
- [7] L. M. Mooney, E. J. Rouse, and H. M. Herr, "Autonomous exoskeleton reduces metabolic cost of walking," *Conference proceedings : ... Annual International Conference of the IEEE Engineering in Medicine and Biology Society. IEEE Engineering in Medicine and Biology Society. Annual Conference*, vol. 2014, no. May, pp. 3065–3068, 2014.

- [8] J. C. Perry, J. Rosen, and S. Burns, "Upper-limb powered exoskeleton design," *IEEE/ASME Transactions on Mechatronics*, vol. 12, no. 4, pp. 408–417, 2007.
- [9] A. M. Dollar and H. Herr, "Lower Extremity Exoskeletons and Active Orthoses: Challenges and State-of-the-Art," *IEEE Transactions on Robotics*, vol. 24, no. 1, pp. 144–158, 2008.
- [10] S. Dhandra, A. Singla, and G. S. Virk, "A Brief Review on Human-Powered Lower-Limb Exoskeletons," *Conference on Mechanical Engineering & Technology (COMET'16)*, no. April, 2016.
- [11] S. Viteckova, P. Kutilek, and M. Jirina, "Wearable lower limb robotics: A review," *Biocybernetics and Biomedical Engineering*, vol. 33, no. 2, pp. 96–105, 2013. [Online]. Available: <http://dx.doi.org/10.1016/j.bbe.2013.03.005>
- [12] M. P. de Looze, T. Bosch, F. Krause, K. S. Stadler, and L. W. O'Sullivan, "Exoskeletons for industrial application and their potential effects on physical work load," *Ergonomics*, vol. 0139, no. December, pp. 1–11, 2015. [Online]. Available: <http://www.tandfonline.com/doi/full/10.1080/00140139.2015.1081988>
- [13] N. Sylla, V. Bonnet, F. Colledani, and P. Fraisse, "Ergonomic contribution of ABLE exoskeleton in automotive industry," *International Journal of Industrial Ergonomics*, vol. 44, no. 4, pp. 475–481, 2014.
- [14] Eurostat, *Health and safety at work in Europe (1999/2007)*, 2010. [Online]. Available: <http://ec.europa.eu/eurostat/documents/3217494/5718905/KS-31-09-290-EN.PDF/88eef9f7-c229-40de-b1cd-43126bc4a946>
- [15] A. A. Shabana and R. Basch, "Multibody System Modeling of Leaf Springs," *Journal of Vibration and Control*, vol. 10, pp. 1601–1638, 2003.
- [16] T. Nef, M. Guidali, and R. Riener, "ARMin III arm therapy exoskeleton with an ergonomic shoulder actuation," *Applied Bionics and Biomechanics*, vol. 6, no. 2, pp. 127–142, 2009. [Online]. Available: <http://content.iospress.com/doi/10.1080/11762320902840179>
- [17] M. . Everling, "Inaccurate load compensation force during fast goal-directed elbow flexion," *Repository TU Delft*, 2017.

APPENDIX I
FLOWCHART OF RESEARCH

This Appendix contains plots of the tests and experiments I did to construct my model and experimental setup together with simulation data that was used to check assumptions.

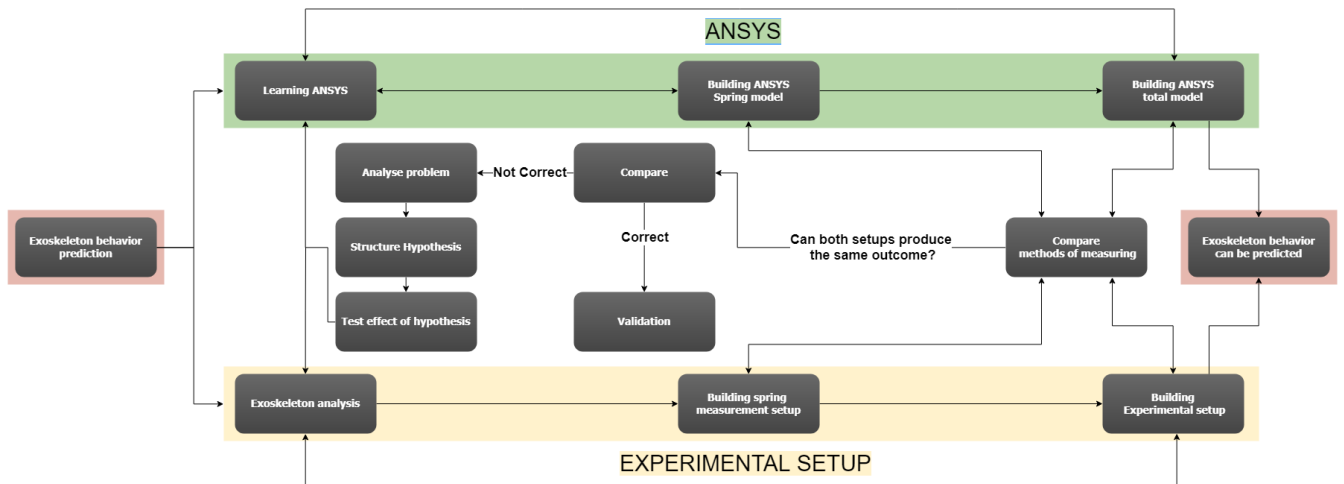


Fig. 14: Flowchart of research iteration steps

This thesis was approached as the flowchart in figure 14 describes. This research consists of two parallel tracks, the ANSYS model and experimental setup. The steps that were iterated the most were learning ANSYS and analyzing the exoskeleton system. After analyzing the exoskeleton the spring model was built first. When building the model and setup, the measurability had to be taken into account of both the ANSYS model and the experimental setup. Some loading types are not possible in ANSYS and some values are difficult to measure in the experimental setup. This had to be in tune. After the methods of measuring were similar, the data could be compared. If the experimental data was consistent enough, the ANSYS settings were investigated and sensitivities of these settings were checked. If the ANSYS model did not provide a comparable outcome, the problem was analyzed, a hypothesis of the problem was constructed and then the adaptation of the ANSYS model was implemented. These steps were repeated until the behavior of the model was similar to the experimental setup in a way that the outcome could be predicted with different loading conditions within the scope. After the spring model was validated the total ANSYS model was developed in the same fashion. The total model and the total experimental setup were created in parallel however the method of measuring was complex as consistent data could not be obtained. Therefore, both setups were altered and the "human" input arm was implemented. This addition provided a method so that the data could be compared. Multiple joint constraints and loading conditions were tested to come up with the correct movement and behavior of the exoskeleton system. This was an iterative process constructing different hypothesis when the model gave an incorrect response until the ANSYS model of the exoskeleton system described the same motion as the experimental setup.

	DEC	JAN	FEB	MAR	APR	MAY	JUN	JUL
Analyse system								
Learn ANSYS								
Build Spring setup								
Build Spring in ANSYS								
Compare ANSYS spring with Spring setup								
Build total model								
Build total setup								
Write program to extract sensor data								
Compare ANSYS with Experimental force curve								
Look for trend lines and combine data into a prediction of the force curve								
Write paper								

Fig. 15: The amount of time spent on different parts of the project

APPENDIX II SPRING SETUP

The experimental setup have evolved over time. First the spring setup was built to check the behavior of the springs, as these elements provide the force in the exoskeleton. A method to compare was developed so that both the ANSYS model and the experimental model were providing similar data.

For the ANSYS model a vertical displacement of the spring tip was implemented that was in line with gravity. The reaction force due to this displacement was the output variable of this simulation. In order to measure the same variables in the experimental setup, a load cell was used to track the force applied at the tip of the spring. Next to that, displacement had to be measured in the experimental setup. A raster board was created so that the displacement could be tracked. This however, was not accurate at all.

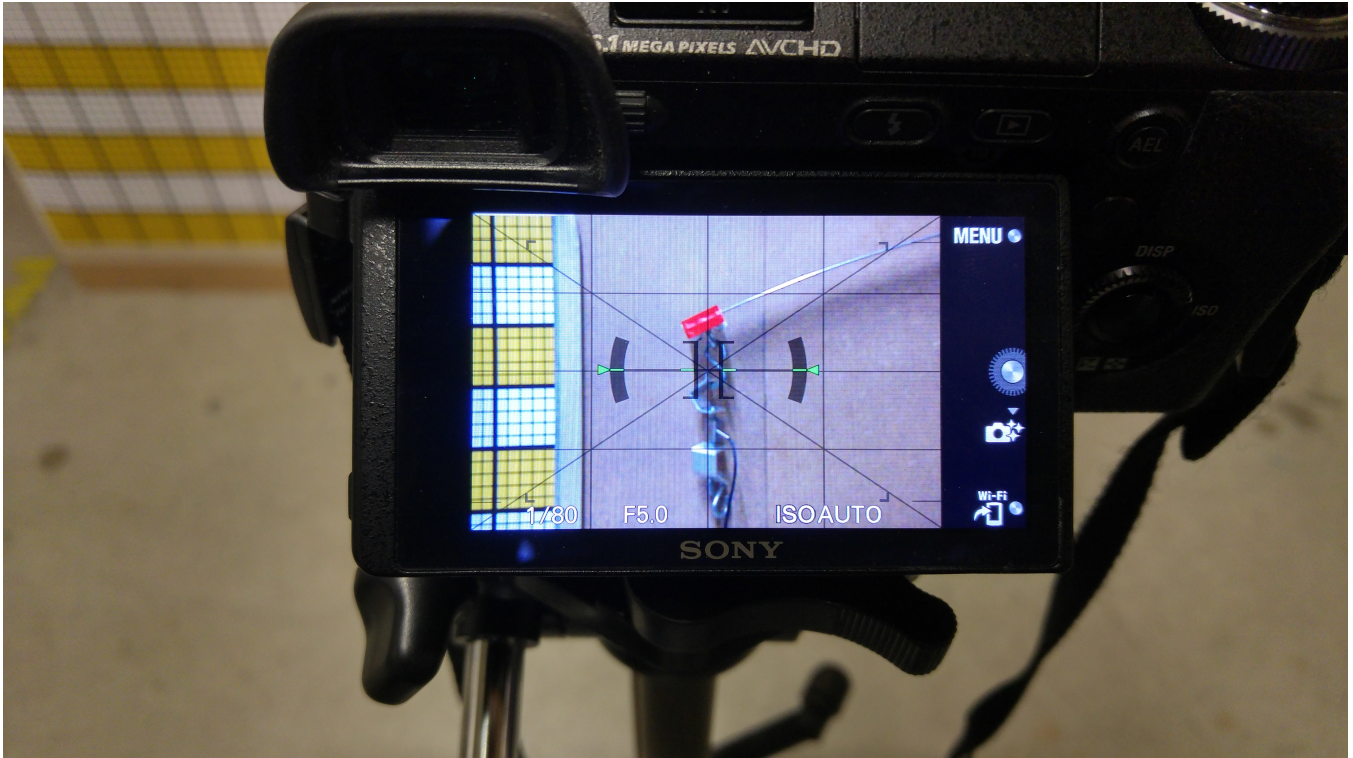
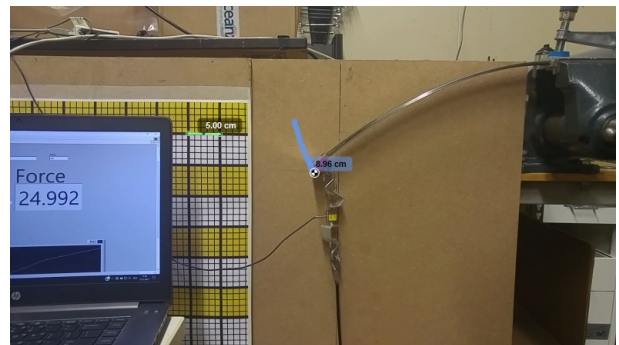
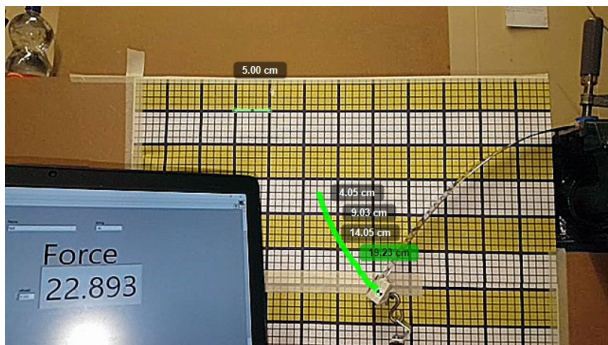


Fig. 16: Camera setup which data is used to analyze in Kinovea

Therefore, the tracking software of Kinovea was used to track the displacement of the tip of these curved springs. Videos were made as the input for Kinovea (Figure 16). First of all, the path of the springs were investigated to make sure that the spring would make the same curve and amount of displacement as the ANSYS model. This is a function of the geometry of the springs. Therefore, the springs were drawn from a photo and implemented into Solidworks. The tracking software however, had a lot of trouble tracking the correct path. It was found that the raster background was too busy for Kinovea. Also the marker at the tip of the springs that Kinovea had to follow had evolved. First the marker was made as a white square at the tip with a black dot on it. This was having trouble as the was very sensitive for shadows. Therefore, it evolved into a red square with a white dot in the corner of square where the end of the springs are located. When the path could be tracked correctly, it was also found that the angle in which it was clamped made a significant different because the of the length of the spring. Therefore, a level was used to make sure that the fixed base of the spring was positioned accordingly.

Now that the shape of the springs was confirmed, the force was measured as a function of the displacement. The data of the force sensor and the Kinovea software were not synchronized. Therefore, the force was displayed on the screen and as well as the total amount of displacement that was provided by Kinovea. The data that could be exported from the tracking software were the x and y displacement coordinates (figure 17). With the total amount of displacement and the Pythagoras Theorem a program was written in Matlab to extract the right y-displacement for the amount of force. This was done multiple times to create an average of this data which was compared with the same amount of displacement of the springs in ANSYS (figure 18).



(a) First spring setup, with manual tracking of the spring tip

(b) Last spring setup, with automatic tracking of the spring tip

Fig. 17: Experimental setup for spring validation

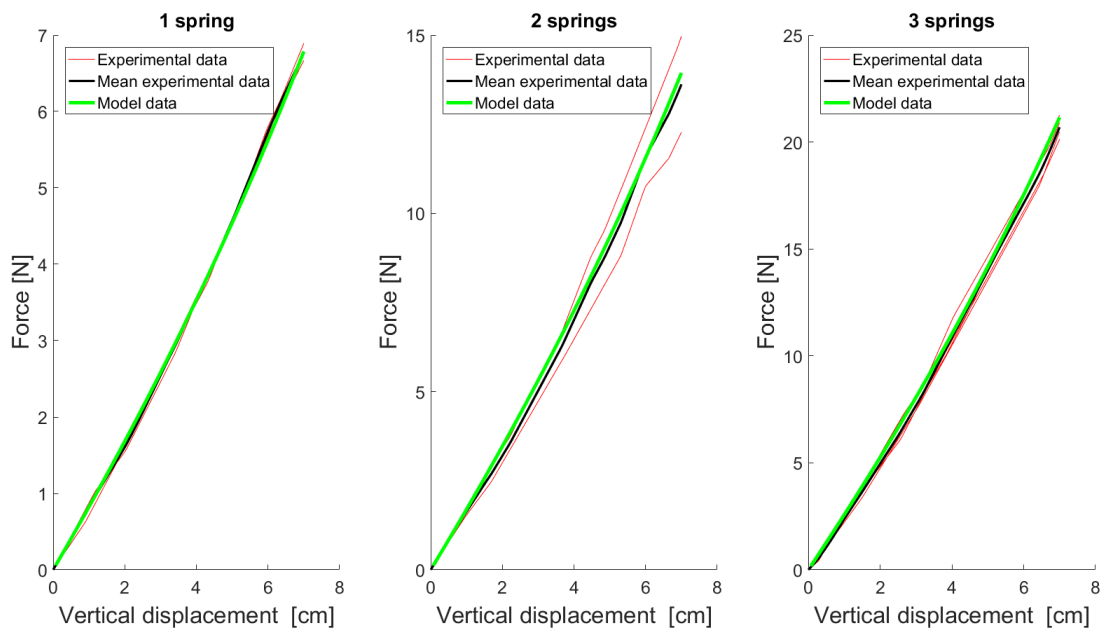


Fig. 18: Spring deflection comparison of the mean of the experimental values with the model value

Figure 18 shows the experimental data together with the model data. The mean of the experimental data is then shown and compared to the model data. The comparison itself can be seen in the paper in figure 8

APPENDIX III TOTAL MODEL SETUP

The total model had to be built after the springs were tested. In order to get the system to move stably, the input arm was developed. The location of the shoulder joint needed to be constructed. An aluminum bar was used that was rotated with the long side of the bar in the loading direction. In this orientation the structure was therefore stiff. The input arm was connected to the arm cup. This arm cup is normally used as the attachment to the human arm. However, this was not a stable and correct connection when testing the system without the human arm. The location of the shoulder joint was also colliding with the springs when loaded as can be seen in figure 19b. This was also happening in the simulations however, in the simulation the spring could just move through the shoulder as it was not defined as a contact point. This gave some positive feedback about the simulation, however this collision needed to be solved in the experimental setup. The first experimental data that was collected was also collected using Kinovea. Kinovea was used to track the angle of the input arm (Figure 20). These initial tests could be done using the vertical spring constraint. This already gave insight that it would improve the fit as the shoulder joint was not touched with this configuration. In this stage of the project, it was already noticed that the hysteresis loop was significantly high. The down movement of the arm required significantly more force than when the arms were moved up.



(a) First total experimental setup



(b) Problem of the first total setup: collision with input arm

Fig. 19: Experimental setup for spring validation of the original system with input arm

In the last setup, which can be seen in figure 9, the shoulder joint location was shifted to the side connected again by an aluminum bar with the long side in the loading direction. Furthermore, the constraint of the input arm and the exoskeleton arm was improved. The connection was given 3 DOF so that unexpected movement could be eliminated.

Moreover, roller and thrust bearings were used to reduce the friction of the shoulder joint. The input arm was attached to the axis so that a potentiometer could be attached to measure the force. A program had to be written in a program called Labview to collect the data of the force- and the potentiometer. Also the sensors had to be calibrated using this program and saved in a single file so that the angle and force were synchronized.

The amount of hysteresis was tested with this new setup to check the hysteresis in the added input arm (which is not part of the actual exoskeleton system)(Figure 21). The hysteresis in this arm was considered low as the total hysteresis is significantly higher. Therefore, the other friction in the system is located in the exoskeleton itself.

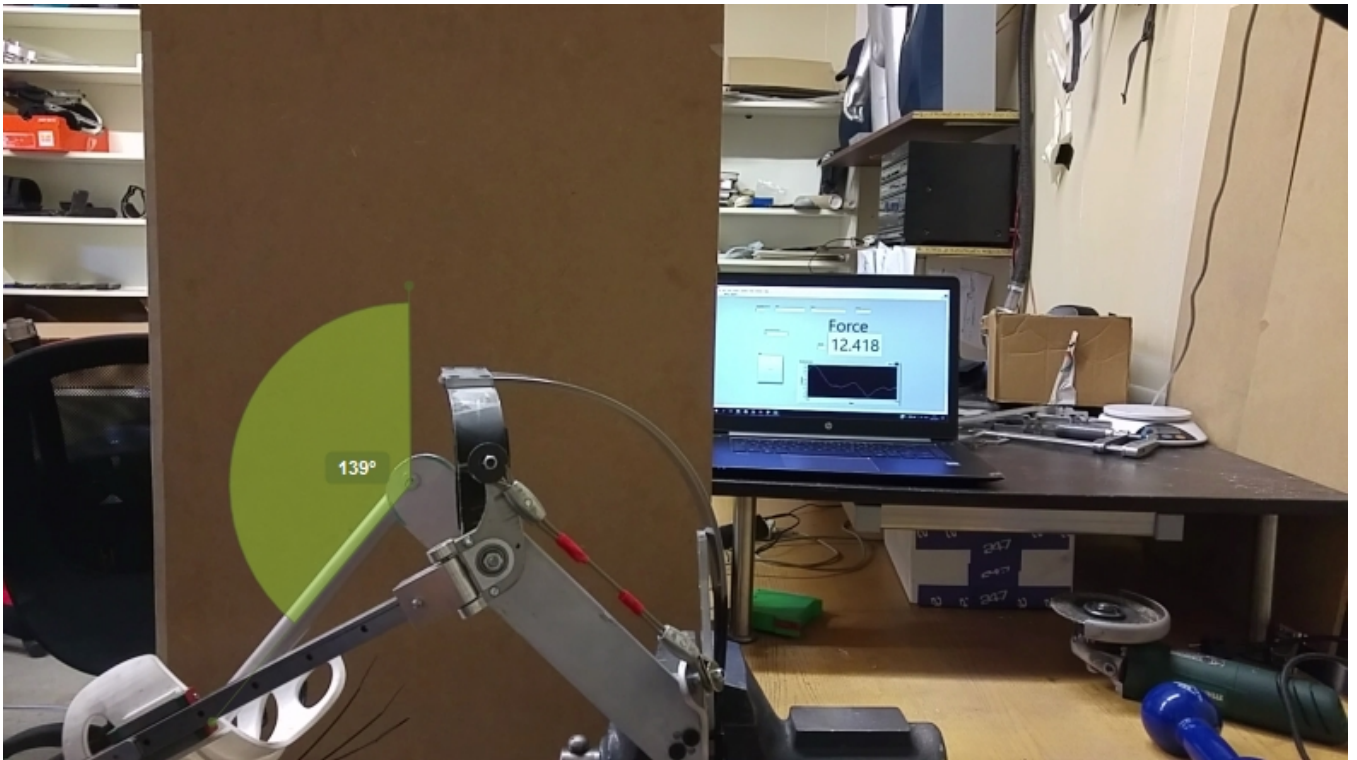


Fig. 20: This was a setup where the force was measured with a load cell and the Angle of the input arm was tracked with Kinovea.

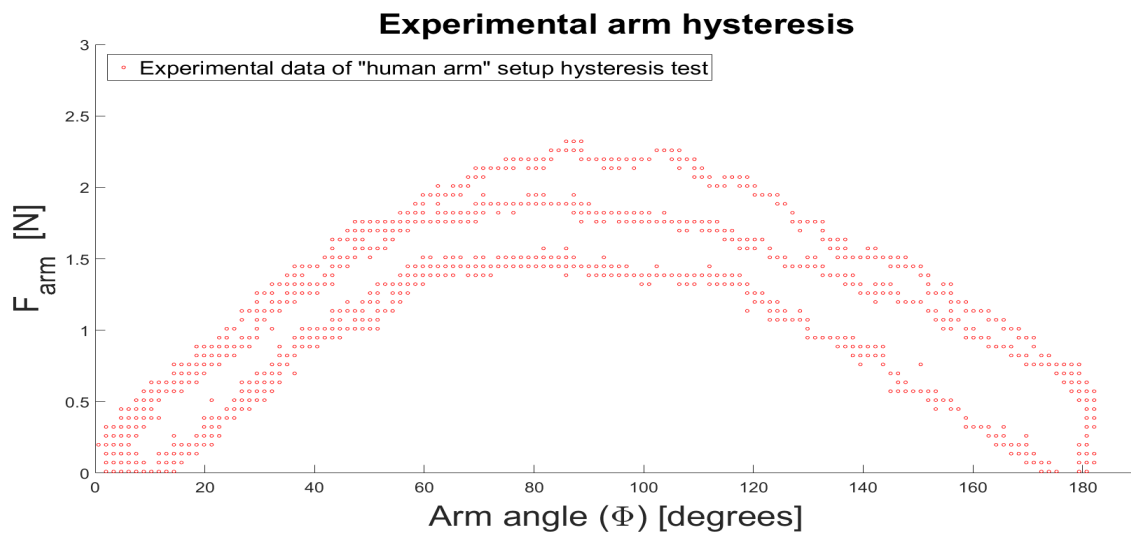


Fig. 21: Testing the amount of hysteresis in the last setup that was generated due to the input arm. It can be seen that this is a low amount compared to the total amount of hysteresis

APPENDIX IV ANSYS SETUP

The spring setup was created first by measuring the initial deflection of the spring. The distance of the two ends of the spring were measured as well as the deflection of the center of the spring. In that way the spring could be modeled as part of a circle. This however, was found to be an invalid assumption. Therefore, the spring was photographed and imported in Solidworks. In that way, the shape of the spring could be exactly drawn from this photo. A scale was also imported in this picture to get the correct size of the spring. The picture was scaled so that it matched the same dimension in Solidworks. With this drawing the upper side of the spring did not fit the bottom side of the other spring when the springs were stacked. The springs were mated in a way that no collision between the springs was present.

The total model was built in Solidworks. The total exoskeleton was measured so that the joint locations and lengths were correct. At first, the hinge after the shoulder hinge, that connects the shoulder hinge and the rails was fixed. This was done because no out of plane motion of the input arm was assumed for this thesis. It was found that this degree of freedom was not only necessary to cope with movement of the human arm in out of plane motion, this DOF is necessary to cope with the out of plane motion of the spring itself. This out of plane motion of the spring is always present, even when the arm is making an in plane motion.

Furthermore, different constraints were tested with the shoulder piece. The fixed constraint of the bottom of the springs were also tested. The springs were attached to the ground with a revolute joint with a high stiffness to see how sensitive the system was to this constraint. The mesh was tested different meshes with different shapes and sizes. Also the total model was meshed to see how much energy was wasted due to bending of the other components in the system. Moreover, the distance between the rails block and the human arm was slightly varied which altered the angle of the rails at the shoulder hinge point. Friction between the springs at different locations was added, and the total amount was altered. Point masses were added at different locations to investigate the effect of gravity.

This all however did not have a drastic effect on the total amount force when the correct shape of the spring could be created with the constraints.

Figure 22 shows the setup of the ANSYS model.

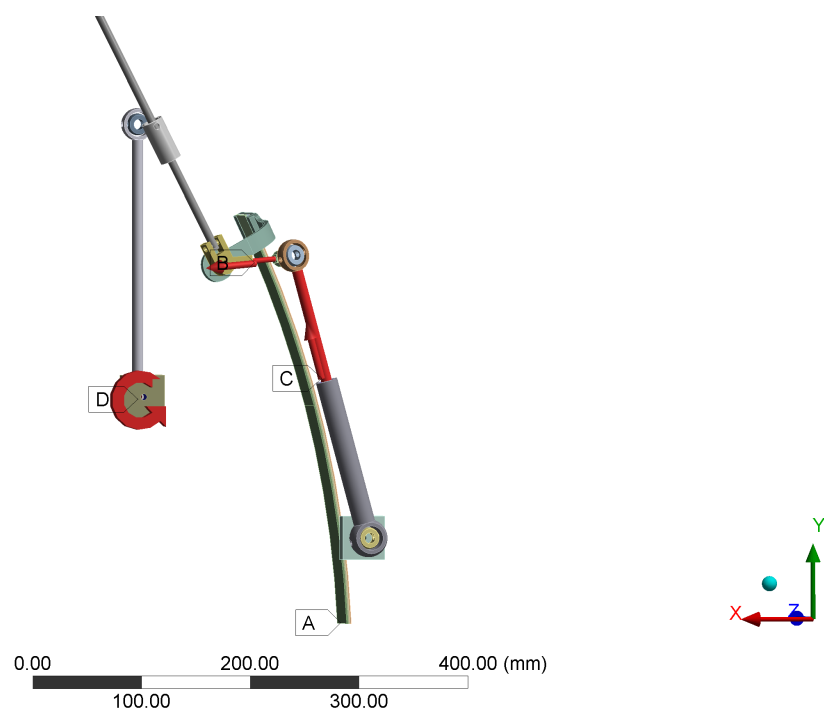


Fig. 22: ANSYS model that was used to predict the force curve. The cable length, lever arm length and the vertical spring constraint could be adjusted in this model. Arrow A is the position where the springs are fixed. The other arrows are the joint displacements. Joint C and B are the joint displacements of the cable length and the lever arm length and joint D is the rotation of the input arm. The link that is connected to the ground at link C is the input arm. This arm has the same length as a human upper arm (from the shoulder joint until the connection point of the exoskeleton, just above the elbow joint)

APPENDIX V
ADDITIONAL FIGURES

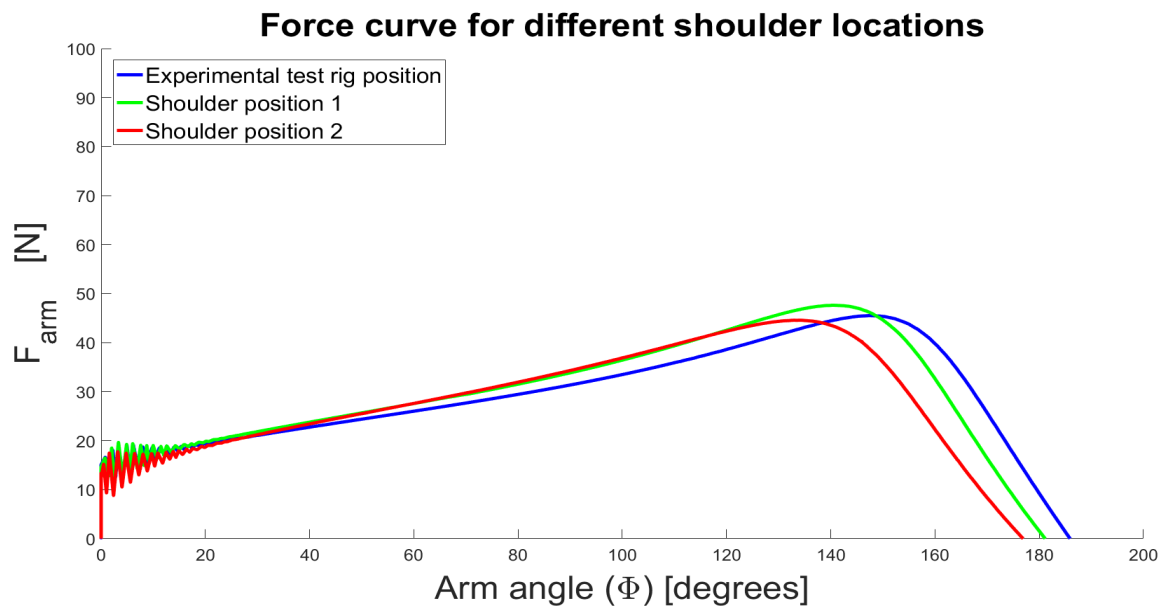


Fig. 23: The shoulder location was also tested. This shifted the force profile, however this changes the location of measurement as well. The force curve therefore remains similar. The locations of the shoulder joint are shifted in the order of 2cm

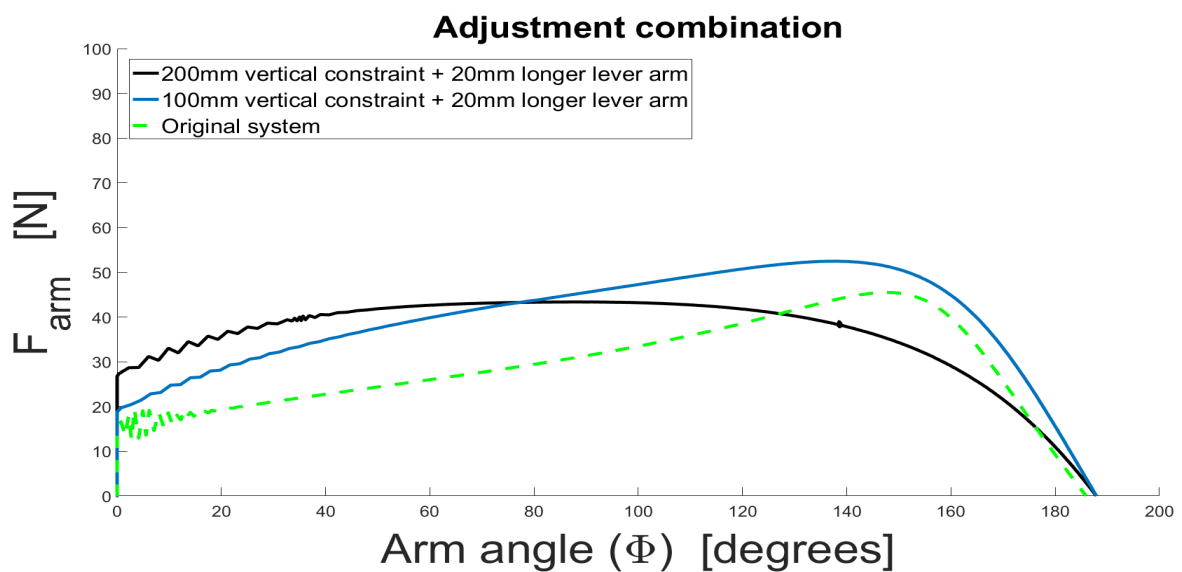


Fig. 24: Combinations that are looked at for different smoothness with a higher force due to the lever arm. A choice can be made were the force should be higher, this can be useful for different applications

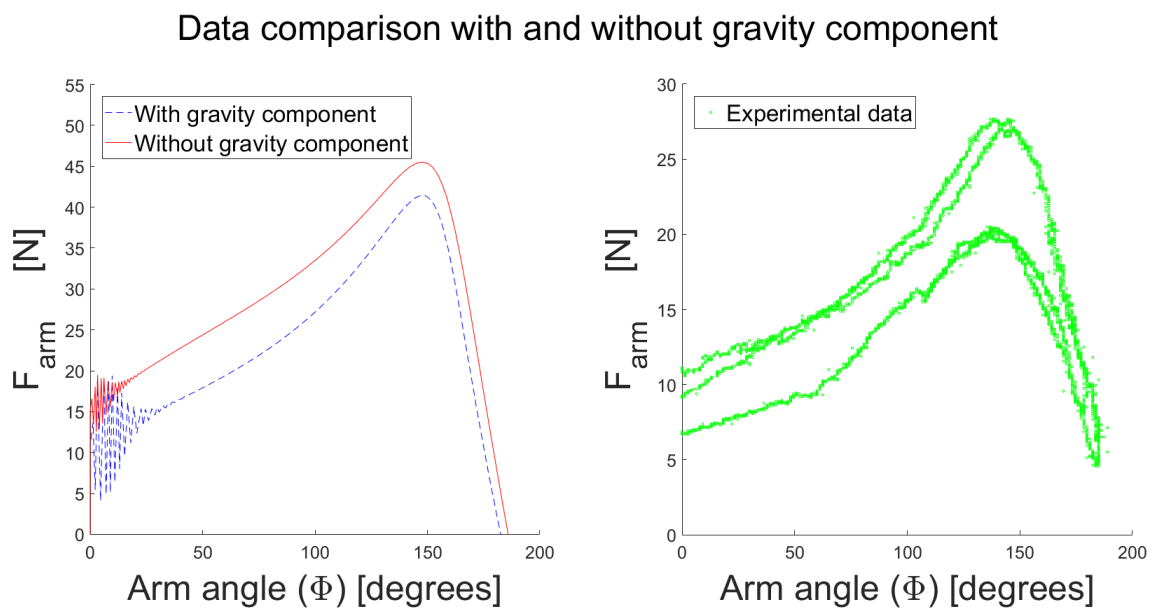


Fig. 25: ANSYS model with and without gravity (first simulations). Different point masses were added in other simulations, however this was not the cause of the scaling factor